Pergamon

Cement and Concrete Research 30 (2000) 937–942

CEMENT AND CONCRETE RESEARCH

Materials characterization of superplasticized cement–sand grout

Marita L. Allan*

Department of Applied Science, Brookhaven National Laboratory, Upton, NY 11973, USA

Received 20 September 1999; accepted 3 April 2000

Abstract

Selected material properties were determined for a superplasticized cement–sand grout formulation designed for sealing boreholes used with geothermal heat pumps (GHPs). The grout was investigated as an alternative to bentonite and neat cements. Hydraulic conductivities (permeability coefficients) of grouts when cast around high density polyethylene (HDPE) pipes to represent a heat exchanger were measured over a range of typical operating temperatures. It was determined that the cement–sand grout had hydraulic conductivity up to two orders of magnitude lower than neat cements depending on test temperature. Infiltration tests performed on grouted tubes containing HDPE pipes also indicated better sealing capability with the cement–sand grout. Mechanical properties measured included bond strength to HDPE, compressive and splitting tensile strength, dynamic and static elastic moduli, shear modulus and Poisson's ratio.

Keywords: Permeability; Bond strength; Elastic moduli; Mechanical properties; Grout

1. Introduction

Superplasticized cement–sand grouts are employed for a wide range of civil engineering applications. These materials have recently been considered for use with geothermal heat pumps (GHPs). Closed-loop GHPs with vertically oriented ground heat exchangers require a grouting material to be placed in the borehole to provide thermal coupling between the U-loop and surrounding media. Fig. 1 is a schematic diagram of a grouted borehole. The bore length is typically 60 to 92 m. The ground serves either as a heat source or heat sink. The temperature of inlet fluid circulating in the U-loop typically ranges from 1°C to 35°C depending on the mode of operation of the GHP. After heat exchange with the surrounding ground, the outlet temperature is several degrees different from the inlet. The grout must also serve as a borehole sealant to protect aquifers from contaminants and maintain heat transfer and hydraulic properties throughout the GHP design life.

Conventional neat cement and bentonite grouts currently used in the USA to backfill boreholes have relatively low thermal conductivities of 0.80 to 0.87 and 0.75 to 0.80 W/m K, respectively [1]. Both materials undergo further reduction of conductivity on drying. Superplasticized cement–sand grouts offer improved thermal conductivity and sealing quality compared with bentonite and neat cement. This results in decreased bore length requirements and reduces the installation costs of GHPs. The material properties determined experimentally for a particular formulation of superplasticized cement–sand grout with a thermal conductivity of 2.42 W/m K are reported in this paper. The grout has been field-tested and is now being used in commercial projects. Further details of the research, including thermal properties, are available elsewhere [2–4]. Information on GHPs can be found in Kavanaugh and Rafferty [5].

2. Experimental

The selected grout was tested for thermal, mechanical, and hydraulic properties. The grout consisted of Type I cement, silica sand, 200-mesh bentonite, water and superplasticizer. The sand had an SiO_2 content of 98.95%. The superplasticizer used was a liquid solution with 42% sodium naphthalene sulphonate by mass. The mix proportions and specific gravity of the superplasticized cement–sand grout (Mix 111) along with neat cement grouts tested for comparison are presented in Table 1. The proportions were devel-

* Tel.: +1-631-344-3060; fax: +1-631-344-2359.
E-mail address: allan@bnl.gov (M.L. Allan).

0008-8846/00/$ – see front matter
PII: S0008-8846(00)00275-1

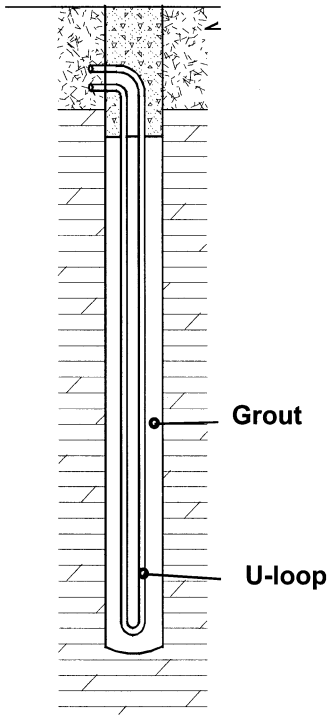

Fig. 1. Schematic diagram of grouted borehole for GHP.

oped on the basis of a number of different considerations that included properties, ease of use by well drillers with simple mixing equipment and economics. The particle size gradation of the sand used and the recommended specification are given in Table 2.

Depending on required quantity, the grouts were either mixed in a planetary mixer or a paddle mixer equipped with a piston pump. The order of addition was water, bentonite, superplasticizer, cement and sand. A paddle mixer was chosen because this is widely used in the US GHP industry and is recommended in a GHP grouting manual [6]. However, it is common practice in other grouting industries to use a high shear grout mixer, particularly for cement–sand grouts. Such mixers may permit omission of bentonite and reduction of water/cement ratio.

2.1. Hydraulic conductivity

The hydraulic conductivity (coefficient of permeability) of the grouts under saturated conditions was measured in a flexible wall triaxial cell permeameter on cylindrical specimens 102 mm in diameter and 70 mm long. The permeant was de-aired tap water at room temperature. The applied pressure gradient was 207 kPa over the length of the specimen. The confining pressure applied to seal a latex membrane to the side surface of the grout specimens was 414 kPa. The experimental set-up followed is that given in ASTM D 5084.

Two series of hydraulic conductivity tests were performed. The first series was on bulk grouts. The second series was on an annulus of grout cast around two axial lengths of 25.4 mm ID (33.0-mm OD) high density polyethylene (HDPE) Driscopipe® 5300 (Phillips 66). The purpose was to represent grout surrounding a U-loop and determine the hydraulic conductivity of the grout/HDPE pipe system. The centre-to-centre separation of the two pipes was 50 mm. The two embedded pipes were sealed with wax before performing hydraulic conductivity tests so that water would flow either through the grout or between the grout/pipe interface. This allowed study of how hydraulic conductivity of the grout/pipe system might be influenced by grout shrinkage and bond quality. A minimum of three specimens per grout mix was tested. All specimens were vacuum saturated with de-aired water prior to measurement. Volumetric flow rates in and out of the specimens were monitored and measurements commenced when equilibrium was reached. All specimens were cast as 204-mm high cylinders and cut to 70 mm with a diamond saw prior to testing. The specimens were cured for 28 days in a water bath.

The effect of thermal mismatch between material components on the system hydraulic conductivity of grout/pipe specimens was investigated. For this purpose, a range of expected operating temperatures was considered. The speci-

Table 2
Sieve analysis of silica sand

	Percentage passing (%)	
Sieve no. (size, μm)	Recommendation	Sand used
8 (2360)	100	100
16 (1180)	95–100	98.84
30 (595)	55–80	66.83
50 (297)	30–55	52.39
100 (149)	10–30	10.75
200 (75)	0–10	0.62

Table 1
Mix proportions of tested cementitious grouts

	Mix 111 cement–sand	Neat cement (w/c = 0.4)	Neat cement (w/c = 0.6)	Neat cement (w/c = 0.8)
Cement (kg/m^3)	587.7	1369	1087	894
Water (l/m^3)	323.3	547.6	652.2	715.2
Sand (kg/m^3)	1251.8	0	0	0
Bentonite (kg/m^3)	6.5	0	0	0
Superplasticizer (l/m^3)	8.8	27.4	0	0
Specific gravity	2.18	1.95	1.74	1.61

mens were first tested at room temperature (21°C). Subsequently, they were conditioned in a water bath for 24 h at 30°C and re-tested. Finally, the specimens were conditioned for 24 h in water kept in a refrigerator at 1°C and hydraulic conductivity was measured for a third time.

2.2. Infiltration rate

Infiltration tests were performed on tubes containing a single U-loop and grouted with either neat cement (w/c = 0.6) or cement–sand grout (Mix 111). The tests involved measuring the change in height of a head of water above each grouted tube. The experimental procedure was similar to that used by Edil et al. [7] in which the sealing characteristics of neat cement and bentonite grouts were compared for water wells. In the present study, four polyvinyl chloride (PVC) tubes 5.1 m long and 102-mm ID were grouted. Two of the tubes were filled with neat cement and the remaining two were filled with Mix 111. In all cases, the grout was tremied from the bottom up into the tubes. After 14 days, the top surface of the grout around the U-loop was made flat and even using a carbide grit blade in a reciprocating saw. The interface between the grout and PVC tubes was sealed with silicone so that flow was restricted to either the grout or the grout/U-loop interface. A 60 cm long, 102-mm ID PVC tube was glued to the top of the grouted tube and filled with water. The infiltration rate calculated was the change in water head divided by time interval.

2.3. Bond strength

The bond strength between cementitious grouts and HDPE was measured by push out tests. An annulus of grout was cast around an axial length of 25.4-mm ID (33.0-mm OD) HDPE Driscopipe® 5300. The diameter of the specimens was 102 mm and the length was 104 mm. The pipe projected out of the grout by 5 mm. Specimens were cured in a water bath for 28 days. Six specimens per grout batch were tested. Movement of the pipe was monitored with a dial gauge and a linear variable differential transducer. The load required to push the pipe out 1 mm was recorded. Bond strength was calculated by dividing this load with the surface area of the embedded pipe. In addition, the effect of temperature on bond strength was investigated by conditioning specimens in water at temperatures of 1°C, 21°C, and 35°C.

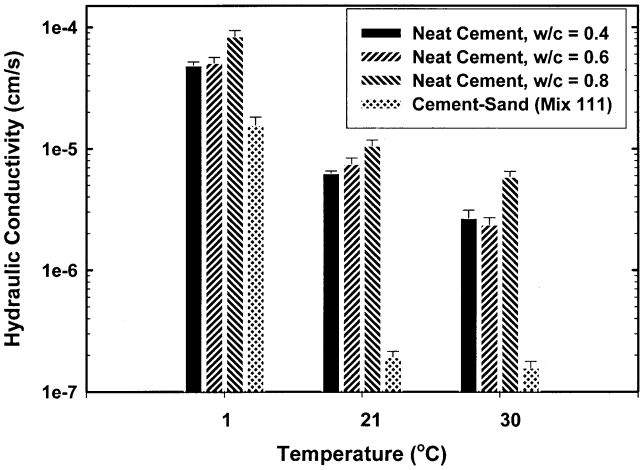

Fig. 3. Hydraulic conductivity for grout/pipe specimens at different temperatures.

2.4. Compressive and splitting tensile strength

Compressive strength tests were performed for the cement–sand grout on six cylindrical specimens, 102 mm in diameter and 204 mm high. The specimens were demoulded after 24 h and wet cured for 28 days. After curing, the specimens were capped and tested in accordance with

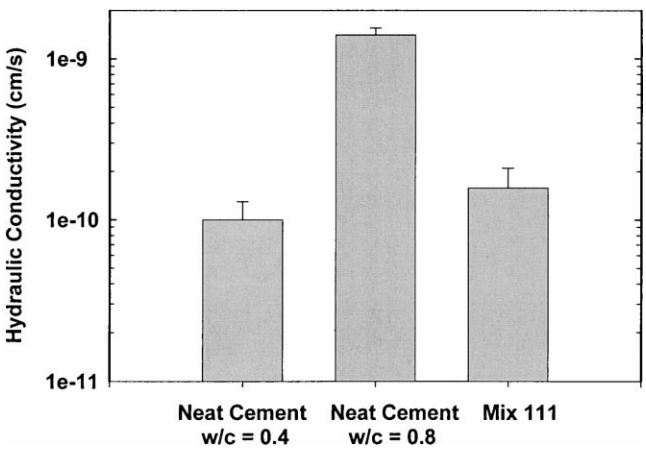

Fig. 2. Hydraulic conductivity for bulk neat cement and Mix 111 cement–sand grouts.

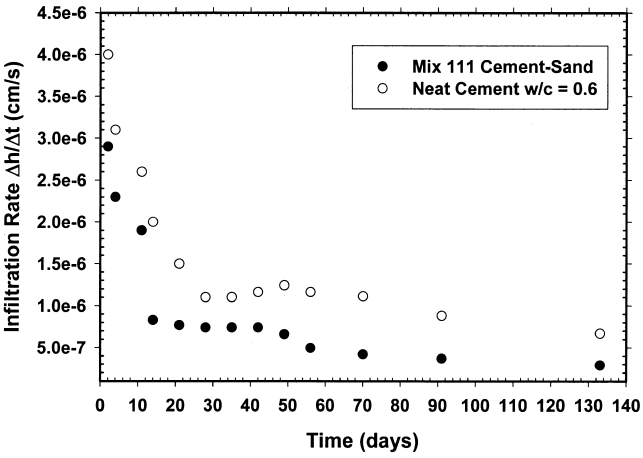

Fig. 4. Infiltration rate vs. time for tubes containing single U-loop and filled with cement–sand or neat cement grout.

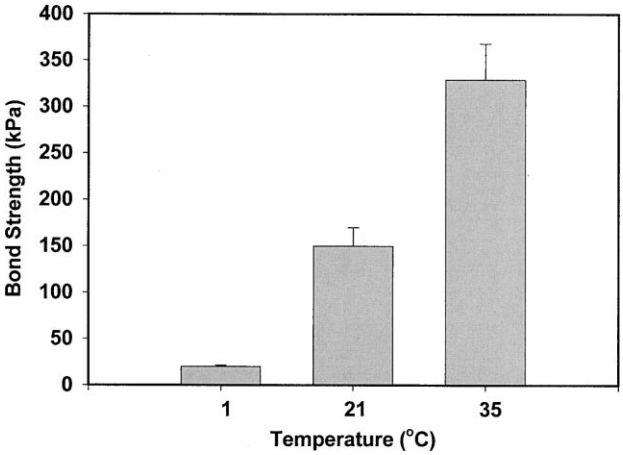

Fig. 5. Bond strength between cement–sand grout and HDPE vs. temperature.

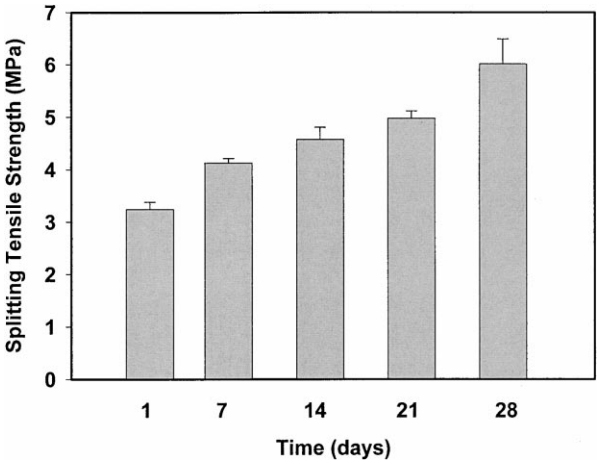

Fig. 6. Splitting tensile strength of cement–sand grout vs. time.

ASTM C 39-86. Cylindrical specimens, 76 mm in diameter and 152 mm high, were used in a series of splitting tensile strength tests. The latter specimens were trimmed to a length of 140 mm and tested following ASTM C 496-90. In addition, the effect of age on splitting tensile strength was evaluated in response to concern that thermal stresses developed in the grout during heat pump operation could cause grout failure, particularly if its strength had not fully developed. Specimens were tested at 1, 7, 14, 21 and 28 days. All cylinders were cured in water except for the group tested at an age of 1 day.

2.5. Elastic and shear moduli and Poisson's ratio

The static elastic modulus and Poisson's ratio of cement–sand grout were measured. A compressometer/extensometer arrangement was employed as described in ASTM C 469. A batch of 11 cylinders, 102 mm in diameter and 204 mm long, were cast and wet cured for 28 days. Each specimen was loaded three times. Measurements taken after the initial loading were used to calculate elastic modulus and Poisson's ratio.

Dynamic properties of the grout were measured in accordance with ASTM C 215. These were elastic modulus, shear modulus, and Poisson's ratio. For this purpose, tests were performed on six beams 205 × 50.8 × 50.8 mm that were wet cured for 28 days. All properties were determined for use in numerical modelling of grout behavior under thermal and dynamic loads.

Table 3
Summary of mechanical properties for Mix 111 cement–sand grout

Compressive strength (MPa)	36.7 ± 4.2
Splitting tensile strength (MPa)	6.01 ± 0.48
Static elastic modulus (GPa)	13.8 ± 0.9
Static Poisson's ratio	0.21 ± 0.02
Dynamic elastic modulus (GPa)	31.8 ± 2.1
Dynamic shear modulus (GPa)	12.7 ± 0.7
Dynamic Poisson's ratio	0.25 ± 0.02

3. Results

3.1. Hydraulic properties

The hydraulic conductivity of bulk cement–sand grout was measured to be $1.58 \times 10^{-10} \pm 5.2 \times 10^{-11}$ cm/s. Fig. 2 compares the hydraulic conductivities for two neat cement grouts and Mix 111. The hydraulic conductivities for the grouts when cast around two lengths of HDPE pipe are depicted in Fig. 3. In the latter figure, hydraulic conductivities at different test temperatures are indicated.

Fig. 4 compares the infiltration rate vs. time between neat cement with w/c = 0.6 and the cement–sand grouts. Each data point represents the average rate for two tubes. The initial two data points were measured over a time interval of 2 days and subsequent points indicate the infiltration rate over a prior 7-day interval.

3.2. Mechanical properties

The bond strengths of grout to HDPE pipe as obtained by push out tests at room temperature were 3.6 ± 0.7 and 150 ± 20.5 kPa for neat cement grout with w/c = 0.4 and cement–sand grout, respectively. The effect of temperature on bond strength is shown in Fig. 5. The remaining measured mechanical properties of the cement–sand grout are summarized in Table 3. The mean value and 1 SD are reported. Fig. 6 depicts the development of splitting tensile strength with age.

4. Discussion

The hydraulic conductivity for bulk superplasticized cement–sand grout was relatively low as indicated in Fig.

2. The mean value was slightly higher than that for the neat cement grout with w/c = 0.4. Predictably, the hydraulic conductivity of the neat cement grouts was influenced by w/c and the mean values ranged from 1.00×10^{-10} to 1.40×10^{-9} cm/s for w/c = 0.4 to 0.8, respectively.

The incorporation of HDPE pipes in the test specimens substantially increased the measured hydraulic conductivity as shown in Fig. 3 and this is attributed to the imperfect physical bonding between the system components. The grout/HDPE interface provides a pathway for fluid flow, thereby resulting in higher system hydraulic conductivities. The results obtained at 21°C demonstrate significantly lower system hydraulic conductivity for the cement–sand grout compared with all of the neat cement grouts. The mean value was 1.93×10^{-7} cm/s for Mix 111, whereas the neat cement grouts had values of 6.3×10^{-6} to 1.06×10^{-5} cm/s for w/c ranging from 0.4 to 0.8, respectively. The lower hydraulic conductivity of the cement–sand grout correlates with observations of the interfacial microstructure that indicated smaller and less continuous gaps between cement–sand grout and HDPE pipe [2,3]. Better bonding is associated with decreased shrinkage and exotherm. It is postulated that thermal expansion of the embedded HDPE pipe occurs during the exothermic period and that subsequent contraction contributes to imperfect bonding. Increased hydraulic conductivity or infiltration rate when cementitious grout is bonded to a dissimilar material has also been reported in other studies [7–9].

The change in system hydraulic conductivity with temperature depicted in Fig. 3 is primarily due to differential thermal expansion and contraction of the HDPE pipe and grout and the resultant changes in dimensions of microannuli at the grout/pipe interface. The coefficient of thermal expansion for the cement–sand grout is 1.65×10^{-5}/°C compared with 1.2×10^{-4}/°C for the HDPE pipe. The performance of the cement–sand grout remained better than that for the neat cement grouts at all test temperatures and, hence, would act as a more effective sealant. At 30°C, all grouts show a reduction in system hydraulic conductivity due to expansion of the embedded pipes and resultant improvement in bonding. Similarly, when the pipes contract at lower temperature, the system conductivities increase. The neat cement grouts with w/c = 0.4 and 0.6 had similar performance throughout the test temperature range. A possible source of error in the results is flow at the HDPE pipe/wax interfaces. However, it is assumed that this effect is similar for all the test materials.

The grout/pipe hydraulic conductivity results at different temperatures were obtained for specimens that were conditioned isothermally. Hence, the effect of different temperatures in the loop legs that would occur in an operating heat exchanger was not taken into account. It is expected that non-uniform thermal loads can induce relative deformations between the grout and the HDPE [4] and this may influence hydraulic conductivity.

Infiltration tests on the grouted tubes containing a U-loop demonstrated that the cement–sand grout has a consistently lower infiltration rate as illustrated in Fig. 4. The mean values after 133 days were 2.9×10^{-7} and 6.7×10^{-7} cm/s for Mix 111 and neat cement with w/c = 0.6, respectively. Infiltration decreased with time for both grouts due to ongoing cement hydration and associated changes in pore structure. Also, since the grouts were not saturated at the commencement of the tests, there may have been some water absorption in the initial stages that contributes to the measured infiltration rates. Current research is investigating grout/U-loop system infiltration rate when hot or cold fluids circulate in the U-loop [10]. These tests will elucidate thermal effects on infiltration rate.

The results of the bond strength tests at room temperature show that cement–sand grout with the mix proportions used has superior bonding characteristics to neat cement with w/c = 0.4. This is attributed to the higher shrinkage and exotherm of neat cement grout. Fig. 5 shows that the bond strength of the cement–sand grout to HDPE pipe is significantly reduced at low temperatures due to contraction of the pipe. At elevated temperature, the bond strength increases as the pipe expands. Therefore, the mechanical bonding characteristics are strongly temperature dependent.

The cement–sand grout has similar compressive strength to concrete with the same w/c. The splitting tensile strength predictably increases with age as shown in Fig. 6 and the strength at 1 day is 54% of that at 28 days. Finite element analysis suggests development of localized tensile stresses in the grout surrounding the U-loop along the axis of symmetry when heat is rejected into the ground [4]. These stresses are unlikely to cause failure for the thermal conditions and grout considered.

The mean static modulus of elasticity of 13.8 GPa measured on the grout compares with 14 to 42 GPa for normal weight concrete and 7 to 28 GPa for cement paste [11]. The dynamic elastic modulus was significantly higher than the static value. The phenomenon of higher modulus obtained by vibration rather than compressive loading is also found for concrete and attributed to lack of induced microcracking and creep [12]. The static Poisson's ratio for the grout was within the typical range for concrete. A higher value was obtained by the dynamic method for the same reason that the dynamic modulus was higher [12]. The mechanical properties may change with in situ curing conditions and operational temperature and this needs to be taken into consideration when modelling and predicting grout performance.

5. Conclusions

Superplasticized cement–sand grout of the mix proportions tested has performance advantages over neat cement when used to fill boreholes used with GHPs. In addition to higher thermal conductivity, the grout exhibits better phy-

sical and mechanical bonding characteristics to HDPE pipe that is used in constructing ground heat exchangers. Enhanced bonding further facilitates heat transfer and also reduces the hydraulic conductivity and infiltration rate of the grout/HDPE system. Such properties are of prime importance for environmental evaluations. Bond strength and system hydraulic conductivity vary markedly throughout the typical operating temperature range due to differences in coefficients of thermal expansion between the materials. The material properties obtained in this study provide input for modelling response to thermal, static, and dynamic loads.

Acknowledgments

This work was supported by the US Department of Energy Office of Geothermal Technologies and performed under contract number DE-AC02-98CH10886. Sincere thanks are expressed to Dr. A.J. Philippacopoulos for beneficial assistance and discussions during this project.

References

[1] M.L. Allan, S.P. Kavanaugh, Thermal conductivity of cementitious grouts and impact on heat exchanger length design for ground source heat pumps, Int J HVAC&R Res 5 (2) (1999) 87–98.

[2] M.L. Allan, Thermal Conductivity of Cementitious Grouts for Geothermal Heat Pumps: FY 1997 Progress Report, BNL 65129, November, 1997.

[3] M.L. Allan, A.J. Philippacopoulos, Thermally Conductive Cementitious Grouts for Geothermal Heat Pumps: FY 1998 Progress Report, BNL 66103, November, 1998.

[4] M.L. Allan, A.J. Philippacopoulos, Performance characteristics and modelling of cementitious grouts for geothermal heat pumps, World Geothermal Congress 2000, in press.

[5] S.P. Kavanaugh, K. Rafferty, Ground Source Heat Pumps: Design of Geothermal Systems for Commercial and Institutional Buildings, ASHRAE, Atlanta, 1997.

[6] F. Eckhart, Grouting procedures for ground-source heat pump systems, Oklahoma State Univ, Ground Source Heat Pump Publ.

[7] T.B. Edil, M.M.K. Chang, L.T. Lan, T.V. Riewe, Sealing characteristics of selected grouts for water wells, Ground Water 30 (3) (1992) 351–361.

[8] C.E. Kurt, R.C. Johnson, Permeability of grout seals surrounding thermoplastic well casing, Ground Water 20 (4) (1982) 415–419.

[9] L.D. Wakeley, D.M. Roy, M.W. Grutzeck, Cementitious mixtures for sealing access shafts/boreholes through evaporite and clastic rocks in a radioactive waste repository, in: C.M. Jantzen, J.A. Stone & R.C. Ewing (Eds.), Scientific Basis for Nuclear Waste Management, vol. VIII, Materials Research Society, Pittsburgh, 1985, pp. 951–958.

[10] M.L. Allan, A.J. Philippacopoulos, Properties and Performance of Cement-Based Grouts for Geothermal Heat Pump Applications: Final Report, BNL 67006, November, 1999.

[11] S. Mindess, J.F. Young, Concrete, Prentice-Hall, Englewood Cliffs, NJ, 1981.

[12] A.M. Neville, Properties of Concrete, 4th edn.Wiley, New York, 1996.